

Pareto Optimal Design of Passive and Active Vehicle Suspension Models

M. J. Mahmoodabadi* & S. M. Mortazavi Yazdi

Department of Mechanical Engineering,
Sirjan University of Technology, Sirjan, Iran
E-mail: Mahmoodabadi@sirjantech.ac.ir,
smmortazaviyazdi1988@gmail.com

*Corresponding author

Received: 24 July 2016, Revised: 16 October 2016, Accepted: 23 October 2016

Abstract: It would be difficult to deny the importance of optimization in the areas of science and technology. This is in fact, one of the most critical steps in any design process. Even small changes in optimization can improve dramatically upon any process or element within a process. However, determining whether an optimization approach will improve on an original design is usually a question that its response in this study has led to an optimal design out of an existing car model. First of all, the optimization of a passive car-quarter model has been accomplished by means of a genetic algorithm. This initial optimization gives a figure of points named "Pareto optimum points". Secondly, through selecting a point amongst them, the design of active model has been completed and optimized based on genetic algorithm. Continuing with this thought, a similar process has been also accomplished with a car-half vehicle model with five degrees of freedom. Though the last optimized active model may prove a more reliable efficient design due to the more comprehensive feature related to the degrees of freedom, the results of each optimization should be considered and may supply equally attractive and diverse choices as well. Anyway, let's focus on the final purpose which is to reduce the vibrations as much as possible. This is what is observed through all the optimization jobs in this study. Comparison of these results with those reported in the literature affirms the excellence of the proposed optimal designs.

Keywords: Active suspension system, Genetic algorithm, Multi-objective optimization, Passive suspension system, PID controller, Vehicle vibration model

Reference: Mahmoodabadi, M. J., and Mortazavi Yazdi, S. M., "Pareto Optimal Design of Passive and Active Vehicle Suspension Models", *Int J of Advanced Design and Manufacturing Technology*, Vol. 9/ No. 4, 2016, pp. 59-73.

Biographical notes: **M. J. Mahmoodabadi** received his BSc and MSc in Mechanical Engineering from Shahid Bahonar University of Kerman, Iran in 2005 and 2007, respectively. He received his PhD in Mechanical Engineering in the Guilan University, Rasht, Iran in 2012. He worked for two years in the Iranian textile industries. Furthermore, during his research, he was a scholar visitor at the Robotics and Mechatronics Group, University of Twente, Enchede, the Netherlands for six months. Now, he is an Assistant Professor of Mechanical Engineering at the Sirjan University of Technology, Sirjan, Iran. His research interests include optimization algorithms, optimal and nonlinear control, robust control and numerical computational methods. **S. M. Mortazavi Yazdi** is Mechanical Engineer at the Department of Design and Manufacturing in Shahid Bahonar Copper Industries Co. (CSP), Iran. He received his BSc in Mechanical engineering from Shahid Bahonar University of Kerman, Iran. His current research focuses on Control, Optimization, and Design of Mechanical Components.

1 INTRODUCTION

Dramatic growth of demand for comfort and reliability of vehicles is continuously increasing. The automotive suspension systems divide into three categories: passive, semi-active, and active. As we know, every vehicle should be flexible against the change of applied load and the center of mass. Furthermore, vibrations caused by engines and the motion paths lead to harmful effects and affect drivers' comfort. Hence impacts, shocks and vibrations are what to diminish over passive and active suspension systems by using the multi-objective optimization in this study.

For years, vehicle ride quality has been improved by both passive and active suspension systems [1], [2]. The passive suspension systems employ ordinary dampers to absorb vibration energy. Furthermore, the springs and dampers do not give energy to the suspension system and can only control the motion of the car body and the wheels by restricting the velocity of the suspension [3-5]. Thus, to overcome this drawback, active and semi-active suspension systems are developed which can enhance the ride quality by using the additional power to obtain a response-dependent damper [3, [4], [6].

Some studies showed that the interior vibrations of a vehicle majorly deteriorate the comfort and road holding capability [7-9]. In 1997, Bouazara studied the influence of suspension system parameters on the vehicle vibration model [10]. In the same year, Hrovat used a three-dimensional vibration model instead of the two-dimensional one to get more exact results [11]. Further, Crolla applied a semi-active suspension model for improving the performance of the vehicle [12], and Bouazara and Richard presented their vibration model in three-dimensional space demonstrating that this model has a good estimation of the vehicle behavior [13]. They also studied three types of suspension system (active, semi-active and passive) for an eight-degree of freedom vibration model [14].

In that work, they combined all the performance criteria to form an objective function for a single-objective optimization process. For this purpose, they used weighting coefficients to adjust comfort and road holding capability criteria in the single-optimization design process. Gundogdu designed an optimum system for a four-degree of freedom quarter car seat using Genetic Algorithm (GA) to determine a set of parameters in order to achieve the best performance of the driver's seat [15]. The desired objective was proposed as the minimization of a multi-objective function formed by the combination of not only suspension displacement and tire deflection but also the head acceleration and crest factor, which has not been practiced as usual by designers. Alkhatib et al. applied genetic algorithm to the optimization problem of a linear one-degree of freedom vibration isolator mount

and then extended the method to optimization of a linear quarter car suspension model [16].

In addition, most of the practical engineering problems need to solve the optimization process involving multiple objective functions so that these functions (design criteria) may in turn conflict with each other. The inherent conflicting behavior of such objective functions lead to a set of optimum solutions named Pareto front [17-20]. For instance, Bagheri et al. applied a new multi-objective genetic algorithm to Pareto optimization of a two-degree of freedom passive linear suspension system [21]. Rajeswari and Lakshmi presented the optimized fuzzy logic controller for the active suspension system based on particle swarm optimization [22]. Nariman-zadeh et al., applied a new multi-objective uniform-diversity genetic algorithm (MUGA) with a diversity preserving mechanism to multi-objective optimization of a five-degree of freedom vehicle vibration model [23].

Mahmoodabadi et al. applied a novel combination of particle swarm optimization and genetic algorithm to Pareto optimum design of a five-degree of freedom vehicle vibration model [24]. In [23], [24], new types of optimization algorithms are utilized for a five-degree of freedom vehicle vibration model containing passive suspension. Furthermore, some researchers showed that by using an active suspension and a simple multi-objective optimization, a better model for suspension system could be achieved. Sharifi applied a multi-objective GA to optimize a sliding mode controller for a vehicle suspension system [25]. Vahidi and Eskandarian introduced a predictive control methodology for active vehicle suspension control [26]. Baumal et al. presented an application of genetic algorithms to the design optimization of an active vehicle suspension system [27].

Thoresson et al. applied a gradient-based approximation method for efficient optimization of a vehicle suspension system [28]. Crews et al. applied multi-objective control optimization for semi-active vehicle suspensions [29]. Guo et al., utilized neural network control for a semi-active vehicle suspension with a magnetorheological damper [30]. Eski and Yildirim applied a new robust neural network control system for vibration control of the vehicle active suspension system [31]. Mao and Wang employed delay-dependent control design for a time-delay supercavitating vehicle model [32]. Some researchers dealt with vehicle models with active suspension systems with PID controller [33], [34].

Yagiz and Sakman used a seven-degree of freedom full vehicle model to design a robust controller and to investigate the performance of active suspensions without losing the suspension working space [35]. Therefore, in this paper, a couple of optimal versions of both passive and active suspension systems are designed

step by step. Through this process, the multi-objective genetic algorithm is used for Pareto optimization of these two models with two- and five-degree of freedom. For the first model (the two-degree one), the conflicting objective functions are the sprung mass acceleration and the relative displacement between the sprung mass and the tire that should be minimized simultaneously. Design variables used in its passive model are the vehicle suspension damping coefficient and the vehicle suspension stiffness coefficient. Also, the design variables used in its active model are PID controller coefficients.

For the second model (the five-degree one), the conflicting objective functions considered for minimization are seat acceleration, front tire velocity, rear tire velocity, relative displacement between sprung mass and front tire, and relative displacement between sprung mass and rear tire. Design variables used in its passive model are seat damping coefficient, vehicle suspension damping coefficients, seat stiffness coefficient, vehicle suspension stiffness coefficients, and seat position in relation to the center of mass. As well, the design variables used in its active model are the coefficients of the PID controller. For the second model, various pairs of wise objectives are selected for two-objective optimization process. Furthermore, the superiority of time domain vibration performance of the proposed design points is shown in comparison with those given in literature.

2 MULTI-OBJECTIVE OPTIMIZATION OF THE VEHICLE SUSPENSION MODEL WITH TWO-DEGREE OF FREEDOM

2.1. Passive Model

Fig. 1 shows a passive vehicle suspension model with two degrees of freedom [10]. This model, consisting of a sprung mass jointed to an un-sprung mass, is the most prevalent model in the passive suspension design researches. For a reasonable simplicity, only the vertical direction of the motion is considered to formulate the motion equations, although the vehicle suspension does not exactly have a vertical motion. Further, the tire form is assumed to be perpetually maintained in contact with the road surface.

M_1 , M_2 , K_1 , K_2 , and C_2 respectively stand for tire mass, sprung mass, tire stiffness coefficient, spring stiffness coefficient, and damping coefficient for the vehicle suspension. According to Newton’s second law of motion, the linear differential equations excited by double bumps, shown in Fig. 2, are as follows [10].

$$M_1 \ddot{Z}_1 = K_2(Z_2 - Z_1) + C_2(\dot{Z}_2 - \dot{Z}_1) - K_1(Z_1 - Z) \quad (1)$$

$$M_2 \ddot{Z}_2 = -K_2(Z_2 - Z_1) - C_2(\dot{Z}_2 - \dot{Z}_1) \quad (2)$$

Where Z_1 and Z_2 are vertical displacements, \dot{Z}_1 and \dot{Z}_2 denote the vertical velocities and \ddot{Z}_1 and \ddot{Z}_2 denote the vertical accelerations of tire and sprung mass, respectively. Also, Z introduces the bump excitation of the road, as shown in Fig. 2, and the input values of fixed parameters are those used in [10] as $M_1= 36$ kg, $M_2=240$ kg and $K_1=16000$ N/m. $10000 < K_2 < 16000$

and $500 < C_2 < 2000$ are two design variables to be optimally found based on multi-objective optimization of two different objective functions, namely, sprung mass (seat) acceleration (c), and relative displacement between sprung mass and tire(Z_2-Z_1). To this end, the multi-objective genetic algorithm defined in toolbox of MATLAB software is used for multi-objective design of passive model shown in Fig. 1. A population of 100 individuals with a crossover probability of 0.9, and mutation probability of 0.1 has been used in 1024 generations according to [21].

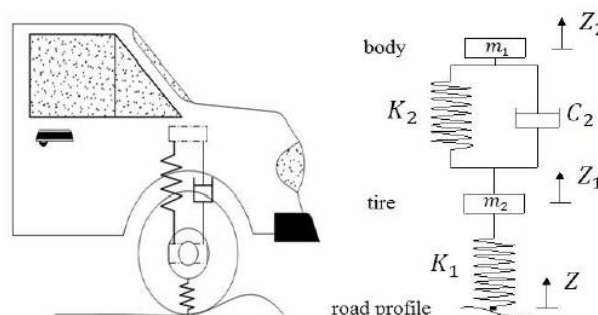


Fig. 1 The Passive vehicle suspension model with two-degree of freedom

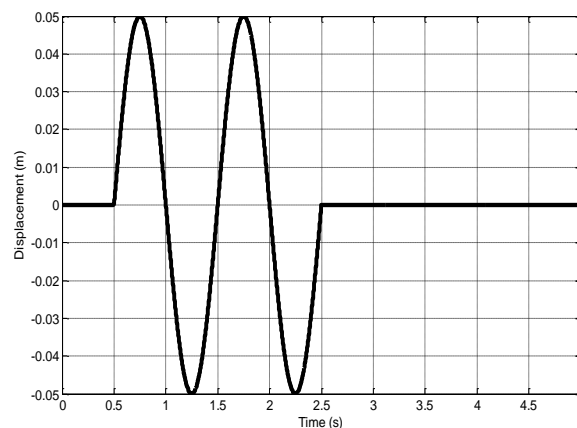


Fig. 2 Bump excitation for vehicle suspension model with two-degree of freedom.

Fig. 3 depicts the Pareto front of the sprung mass acceleration and the relative displacement between sprung mass and tire. It represents different optimum points with respect to these conflicting objectives in the

passive model. Points Land R stand for the best sprung mass acceleration and the best relative displacement between sprung mass and tire, respectively. The selected point indicated in the top-left of the figure is one of the optimum design points which stands for an appropriate position; satisfies both of two conflicting objectives in comparison with the other points.

Table 1 The values of objective functions and their associated design variables for the optimum points shown in Fig. 3

	\ddot{Z}_2 (m/s ²)	$(Z_2 - Z_1)$ (m)	K_2 (N/m)	C_2 (N.s/m)
Point L	3.9103	0.0533	10484.9069	1976.4774
Point R	4.6447	0.0513	15933.8257	1978.1740
Selected point	3.9167	0.0532	10529.8920	1978.1775

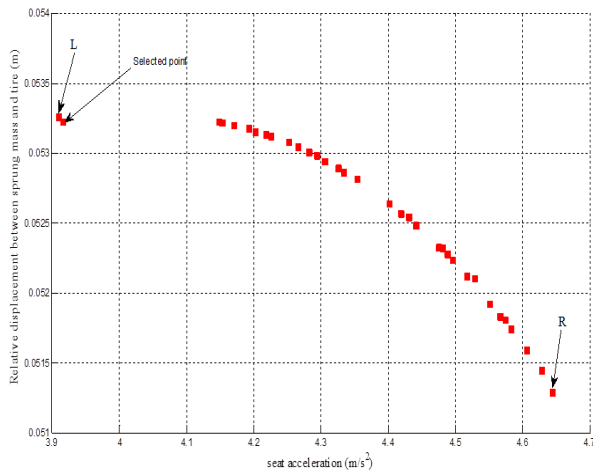


Fig. 3 Obtained Pareto front for the two-degree of freedom passive suspension system using the multi-objective genetic algorithm

The corresponding values of objective functions and design variables of these optimum design points are shown in Table 1. It should be noted that all of the optimum design points in this Pareto front are non-dominated and could be chosen by a designer based on the kind of requirement. The selected point could give an optimum choice to reach to an optimal design of two-degree of freedom passive suspension model. Then, by installing a PID controller and optimization of that, we will reach to an optimum design of the two-degree of freedom active suspension model in the next part.

2.2. Active Model

A two-degree of freedom active vehicle suspension model shown in Fig. 4 adopted from [36] is now considered. This model is composed of a passive suspension and an actuator that is handled by a PID controller. Parameters M_1 , M_2 , K_1 , K_2 , and C_2 are the

same fixed parameters of passive vehicle model whose values were expressed or obtained in the previous section. In fact, $M_1=36$ kg, $M_2=240$ kg and $K_1=16000$ N/m. K_2 and C_2 have the corresponding values of the selected optimum point shown in Fig. 3 ($K_2=10529.82$ N/m and $C_2=1978.17752$ N.s/m). The linear differential equations of motion with regard to the degrees of freedom could be written as follows [36].

$$M_2\ddot{Z}_2 = -K_2(Z_2 - Z_1) - C_2(\dot{Z}_2 - \dot{Z}_1) + u \quad (3)$$

$$M_1\ddot{Z}_1 = K_2(Z_2 - Z_1) + C_2(\dot{Z}_2 - \dot{Z}_1) - K_1(Z_1 - Z) - u \quad (4)$$

Where Z_1 , Z_2 , \dot{Z}_1 , \dot{Z}_2 , \ddot{Z}_1 , and \ddot{Z}_2 denote those same displacements, velocities and accelerations of the passive vehicle model used in the previous section. Also, Z represents the double bumps excitation of the road, as shown in Fig. 2 and u is the PID controller signal. The ideal version of the PID controller is given by the following formula:

$$u = k_p e + k_d \frac{de}{dt} + k_i \int e dt \quad (5)$$

Ideal where u is the control signal and e is the control error ($e=Z_d-Z$). The reference value Z_d is called the desired set point and its value is 0 and Z denotes the relative displacement between sprung mass and unsprung mass, in this paper. A PID controller calculates an error value as the difference between the state variable and the desired set point. The controller attempts to minimize the error by adjusting the process control inputs. The control signal is thus a sum of three terms: a proportional term that is proportional to the error, a derivative term that is proportional to the derivative of the error and an integral term that is proportional to the integral of the error. The controller parameters are then proportional gain k_p , derivative gain k_d and integral gain k_i .

Now, the active model must be optimized to reach the optimum performance of the suspension system. Therefore, similar to the multi-optimization of passive model, the multi-objective genetic algorithm defined in toolbox of MATLAB software is used, but at this time, the active model shown in Fig. 4 is optimized and $-10000 < k_p < -6000$, $-100 < k_d < 1000$, $-100 < k_i < 1000$ are three design variables to be found based on multi-objective optimization of two different objective functions, namely, the sprung mass (seat) acceleration (\ddot{Z}_2) and the relative displacement between sprung mass and tire ($Z_2 - Z_1$). Like the previous section, a population of 100 individuals with a crossover probability of 0.9 and mutation probability of 0.1 has been used in 1024 generations. The initial range of the design variables is $[-10000, 1000]$. These conditions are same with those of the proposed model in [21].

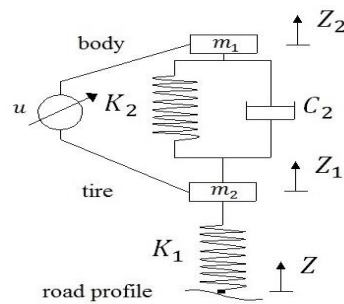


Fig. 4 Two-degree of freedom vehicle model with active suspension

Table 2 The values of objective functions and their associated design variables for the optimum points shown in Fig. 5

Point	\ddot{Z}_2 (m/s ²)	$(Z_2 - Z_1)$ (m)	k_p	k_d	k_i
A	2.822	0.0311	-9987.077	970.991	45.554
B	2.621	0.0369	-9963.036	392.011	159.564
C	2.389	0.0432	-9957.618	-75.965	251.761

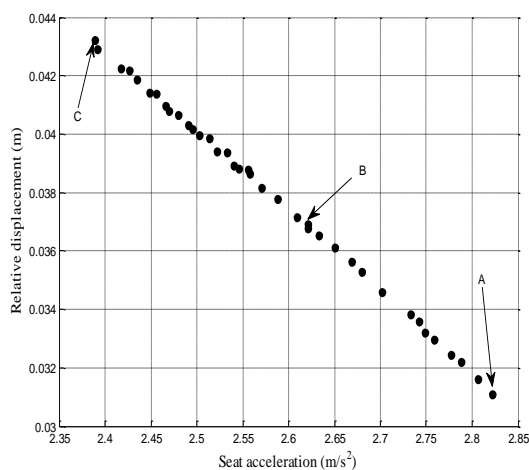


Fig. 5 Obtained Pareto front for the two-degree of freedom active suspension system using the multi-objective genetic algorithm

Fig. 5 depicts the Pareto front of the sprung mass acceleration and the relative displacement between sprung mass and tire. It represents different optimum points with respect to these conflicting objectives in the active model. In this figure, three optimum design points are denoted and the corresponding values of objective functions and their design variables are given in Table 2. It is clear from Fig. 5 that both of the objective functions are optimized to an acceptable level compared to Fig. 3. The comparison of two obtained Pareto fronts with the one proposed in [21] is shown in Fig. 6 and the values of objective functions are given in Table 3. Therefore, the superiority of the proposed optimal active design is clear. The time histories of two objective functions for the

suggested optimum design points by this work and those suggested in [10] and [21] are shown in Figs. 7 and 8. The values of two objective functions for these points are given in Table 3.

Table 3 Objective functions associated with the optimum design points from this work and [10], [21].

	\ddot{Z}_2 (m/s ²)	$(Z_2 - Z_1)$ (m)
Point B, by this work	2.8221	0.03111
Suggested optimum point in [21]	2.6210	0.03692
Suggested optimum point in [10]	2.3892	0.04323

The integral of absolute values the time behaviors of control forces for optimal design points A, B and C (Fig. 5) are 383.2641 N, 381.9616 N, and 428.4899 N (point B has the minimum value) respectively.

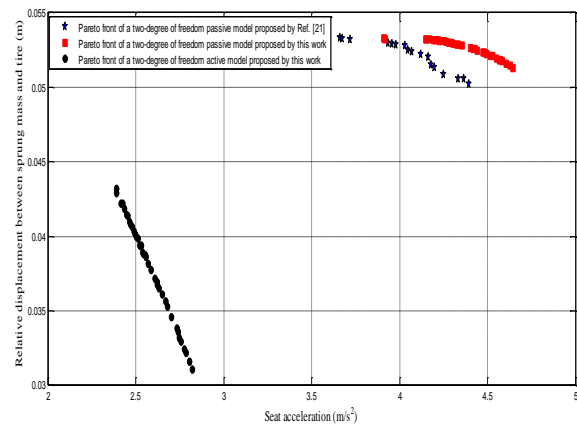


Fig. 6 The comparison of the Pareto fronts obtained by this work and [21] for the two-degree of freedom vehicle model

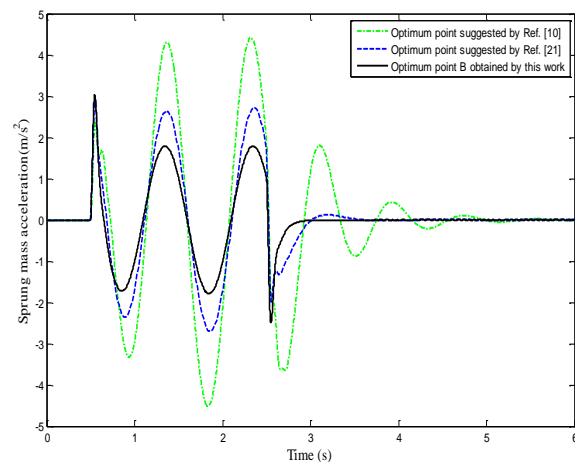


Fig. 7 The comparison of time responses of relative displacement between sprung mass and tire for point B (by this work) and optimum points proposed in [10], [21]

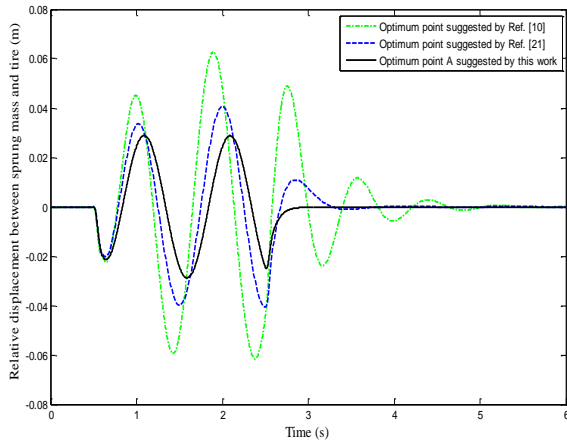


Fig. 8 The Comparison of time responses of sprung mass acceleration for point B (by this work) and optimum points proposed in [10], [21]

3 MULTI-OBJECTIVE OPTIMIZATION OF THE VEHICLE SUSPENSION MODEL WITH FIVE-DEGREE OF FREEDOM

3.1. Passive Model

Fig. 9 shows a passive vehicle suspension model with five degrees of freedom [10]. This model consisting of a sprung mass (body) jointed to three un-sprung masses (tires and seat) not only simplifies the analysis but also includes most of the characteristics of the exact suspension model. It is noteworthy that both passive and active models with five-degree of freedom consider the seat having a linear spring and damper. Further, the tire form is assumed to be perpetually maintained in contact with the road surface.

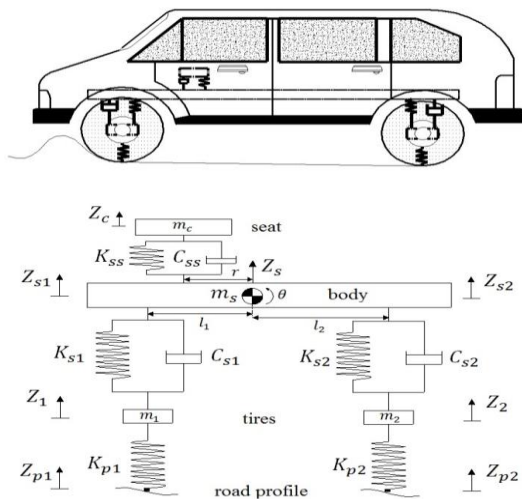


Fig. 9 The Passive vehicle suspension model with five-degree of freedom

In Fig. 9, parameters m_1 , m_2 , m_s , I_s , K_{p1} , K_{p2} , l_1 , and l_2 represent the vehicle's fixed parameters, respectively, front tire mass, rear tire mass, sprung mass, moment of inertia of sprung mass, front tire stiffness coefficient, rear tire stiffness coefficient and the front and rear tires position relative to the center of mass. Design variables K_{ss} , K_{s1} , K_{s2} , C_{ss} , C_{s1} , C_{s2} , and r and r denote seat stiffness coefficient, stiffness coefficients for vehicle suspension, seat damping coefficient, damping coefficients for vehicle suspension and the set position relative to the center of mass, respectively. As well, subscripts 1 and 2 denote tire axes. As shown in Fig. 10, the model is excited by the double bumps. In addition, the linear differential equations of motion are derived from Newton-Euler equations as follows [10].

$$z_{ps} = z_s - r\theta \tag{6}$$

$$z_{s1} = z_s - l_1\theta \tag{7}$$

$$z_{s2} = z_s + l_2\theta \tag{8}$$

$$F_{ss} = K_{ss}(z_c - z_{ps}) + C_{ss}(\dot{z}_c - \dot{z}_{ps}) \tag{9}$$

$$F_{s1} = K_{s1}(z_{s1} - z_1) + C_{s1}(\dot{z}_{s1} - \dot{z}_1) \tag{10}$$

$$F_{s2} = K_{s2}(z_{s2} - z_2) + C_{s2}(\dot{z}_{s2} - \dot{z}_2) \tag{11}$$

$$m_c \ddot{z}_c = -F_{ss} \tag{12}$$

$$m_s \ddot{z}_s = -F_{s1} - F_{s2} + F_{ss} \tag{13}$$

$$I_s \ddot{\theta} = l_1 F_{s1} - l_2 F_{s2} - r F_{ss} \tag{14}$$

$$m_1 \ddot{z}_1 = F_{s1} - K_{p1}(z_1 - z_{p1}) \tag{15}$$

$$m_2 \ddot{z}_2 = F_{s2} - K_{p2}(z_2 - z_{p2}) \tag{16}$$

Where Z_c , Z_s , $Z_{si}(i=1,2)$ and θ are vertical seat displacement, vertical displacement of the central gravity of the sprung mass, vertical displacement of the ends of the sprung mass, and rotating motion (pitching motion), respectively.

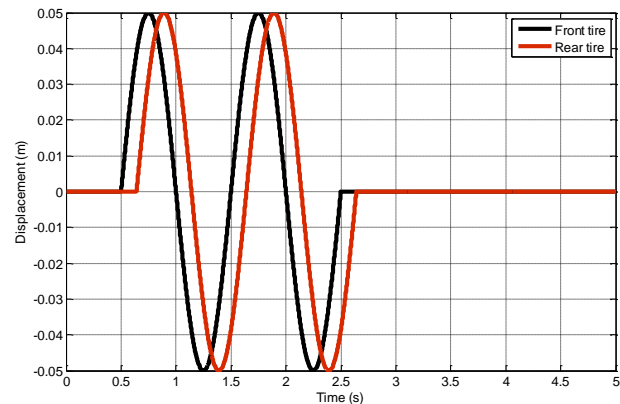


Fig. 10 Double bumps excitation for vehicle suspension model with five-degrees of freedom

In addition, \dot{z}_c , \dot{z}_s and \dot{z}_{si} ($i=1,2$) indicate vertical seat velocity, vertical tire velocity, and vertical velocity of the ends of the sprung mass, respectively. \ddot{z}_c , \ddot{z}_s , \ddot{z}_{si} ($i=1,2$), and $\ddot{\theta}$ denote vertical seat acceleration, vertical acceleration of the center of gravity of the sprung mass, vertical tires acceleration, and rotating acceleration (pitch acceleration), respectively.

Table 4 The values of fixed parameters for the passive model with five-degree of freedom

l_1	1.011 m
l_2	1.803 m
m_1	40 kg
m_2	35.5 kg
m_c	75 kg
m_s	730 kg
I_s	1230 kg m ²
K_{p1}	175500 N/m
K_{p2}	175500 N/m

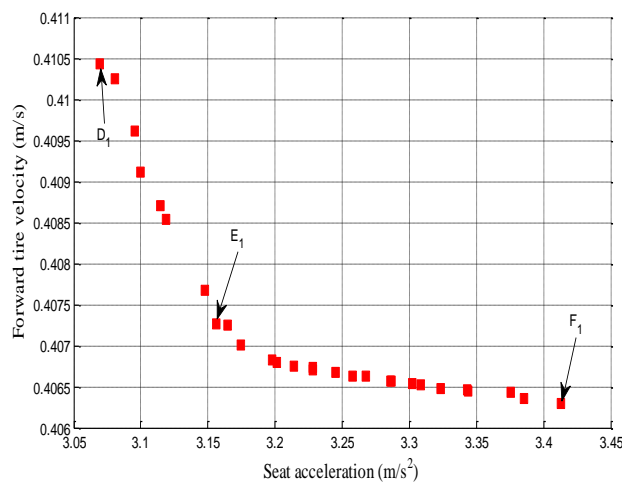


Fig. 11 The Obtained Pareto front of the five-degree of freedom passive suspension for seat acceleration and front tire velocity using the multi-objective optimization genetic algorithm

Finally, z_{p1} and z_{p2} indicate the double bumps excitation of the road, as shown in Fig. 10. It is assumed that the vehicle velocity has the constant value of $v = 20$ m/s over the double bumps and the rear tire moves on the same trajectory of the front tire with a delay of $\Delta t = (l_1 + l_2)/v$. The values of fixed parameters are given in Table 4 with regard to [10]. In this section

$50000 \leq K_{ss} \leq 150000$, $10000 \leq K_{s1} \leq 20000$, $10000 \leq K_{s2} \leq 20000$, $1000 \leq C_{ss} \leq 4000$, $500 \leq C_{s1} \leq 2000$, $500 \leq C_{s2} \leq 2000$ and $0 \leq r \leq 0.5$ are considered as seven design variables to be optimally found based on the multi-objective optimization of five different objective functions, namely, seat acceleration, front tire velocity, rear tire velocity, relative displacement between sprung mass and front tire, and the relative displacement between sprung mass and rear tire.

Table 5 The values of objective functions and their associated design variables of the optimum points shown in Fig. 11

	K_{ss} (N/m)	K_{s1} (N/m)	K_{s2} (N/m)
Point D_1	94013.1805	10156.5046	15942.0000
Point E_1	92041.0331	10159.7081	18589.5539
Point F_1	87208.5102	10212.2502	19021.1269
	C_{ss} (Ns/m)	C_{s1} (Ns/m)	C_{s2} (Ns/m)
Point D_1	2417.7909	1429.9201	1574.5840
Point E_1	2476.8518	1085.9229	1552.6168
Point F_1	2473.9271	1009.5767	691.5997
	r (m)	\ddot{z}_c (m/s ²)	\dot{z}_1 (m/s)
Point D_1	0.49896	3.0697	0.4104
Point E_1	0.4895	3.1648	0.4072
Point F_1	0.4941	3.4130	0.4063

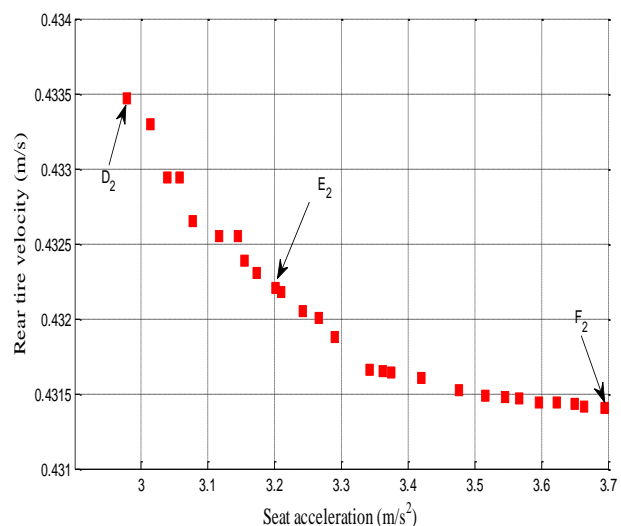


Fig. 12 The Obtained Pareto front of the five-degree of freedom passive suspension for seat acceleration and rear tire velocity using multi-objective optimization genetic algorithm

Table 6 The values of objective functions and their associated design variables of the optimum points shown in Fig. 12

	$K_{ss}(N/m)$	$K_{s1}(N/m)$	$K_{s2}(N/m)$
Point D_2	89163.0239	10192.3170	10705.4247
Point E_2	97209.7539	10249.0677	10534.9070
Point F_2	98382.7617	11202.0151	10517.1537
	$C_{s1}(Ns/m)$	$C_{s2}(Ns/m)$	
Point D_2	3083.7583	1351.8687	1869.0524
Point E_2	2869.4824	1079.7968	1658.3259
Point F_2	2787.2322	1022.8388	1500.4208
	$r(m)$	$\ddot{z}_c (m/s^2)$	$\dot{z}_2 (m/s)$
Point D_2	0.4959	2.9784	0.4335
Point E_2	0.2903	3.2018	0.4322
Point F_2	0.0512	3.6955	0.4314

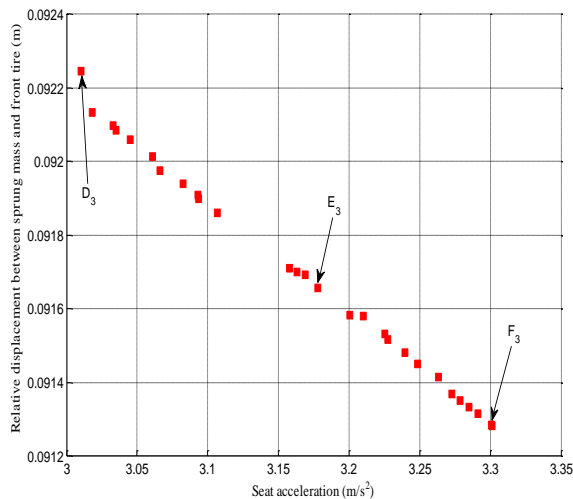


Fig. 13 The Obtained Pareto front of the five-degree of freedom passive suspension for seat acceleration and relative displacement between sprung mass and front tire using multi-objective optimization genetic algorithm

Note that from these five objective functions, four different pairs of them are considered in various two-objective optimization processes in which; The fixed objective is the seat acceleration, and the other one is chosen from the other four objectives. As we know, all of the objective functions must be minimized, simultaneously. For this purpose, similar to previous sections, the multi-objective genetic algorithm defined in toolbox of MATLAB software is used for multi objective design of passive model shown in Fig. 9. A population of 80 individuals with a crossover probability of 0.9 and

mutation probability of 0.1 has been used in 240 generations.

Table 7 The values of objective functions and their associated design variables of the optimum points shown in Fig. 13

	$K_{ss}(N/m)$	$K_{s1}(N/m)$	$K_{s2}(N/m)$
Point D_3	89159.9059	10311.5458	12705.8567
Point E_3	89165.1050	10314.6204	12664.7729
Point F_3	89169.1365	10315.7274	12647.9414
	$C_{s1}(Ns/m)$	$C_{s2}(Ns/m)$	
Point D_3	2571.8137	1964.0384	1485.3474
Point E_3	2567.7195	1966.8788	1476.0882
Point F_3	2566.5456	1967.2258	1469.6132
	$r(m)$	$\ddot{z}_c (m/s^2)$	$d_1(m)$
Point D_3	0.4859	3.0104	0.0922
Point E_3	0.2754	3.1687	0.0917
Point F_3	0.1132	3.3009	0.0913

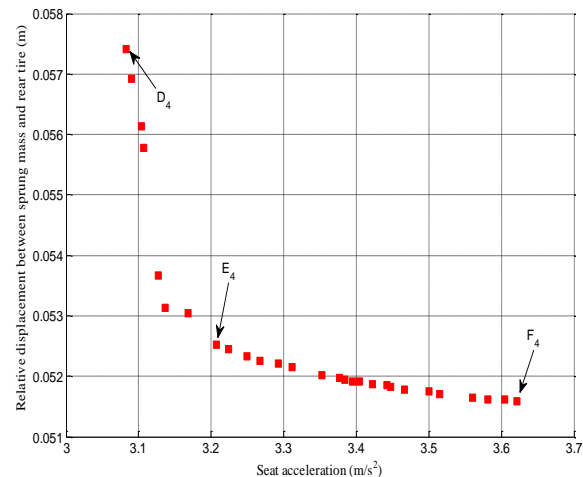


Fig. 14 The Obtained Pareto front of the five-degree of freedom passive suspension for seat acceleration and relative displacement between sprung mass and rear tire using multi-objective optimization genetic algorithm

In Figs. 11 to 14 the Pareto fronts of a five-degree of freedom passive suspension model are depicted. The values of objective functions and their associated design variables of three optimum points in each pairs of objectives are shown in Tables 5 to 8. Design points D_1 , D_2 , D_3 , and D_4 stand for the best seat acceleration (\ddot{z}_c), while points F_1 , F_2 , F_3 , and F_4 represent the best \dot{z}_1 , \dot{z}_2 , d_1 , and d_2 , respectively. From these figures,

it is clear that choosing a better value for any objective function in these Pareto fronts would lead to a worse value of another one. Obviously, there are some important optimum design facts among these objective functions that can be readily observed in that Pareto front. From these design points, the selected points E_1 , E_2 , E_3 , and E_4 satisfy all pairs of objectives in an acceptable level.

Table 8 The values of objective functions and their associated design variables of the optimum points shown in Fig. 14

	$K_{ss}(\text{N/m})$	$K_{s1}(\text{N/m})$	$K_{s2}(\text{N/m})$
Point D_4	102408.7747	10703.5080	14871.9250
Point E_4	111031.7107	10730.5283	19382.8372
Point F_4	112541.8623	10763.5887	19393.2878
	$C_{ss}(\text{Ns/m})$	$C_{s1}(\text{Ns/m})$	$C_{s2}(\text{Ns/m})$
Point D_4	3531.4237	1686.4035	1990.7008
Point E_4	3580.8821	1309.0825	1991.5468
Point F_4	3646.8442	819.7926	1991.6428
	$r(\text{m})$	$\ddot{z}_c \text{ (m/s}^2\text{)}$	$d_2 \text{ (m)}$
Point D_4	0.4997	3.0827	0.0574
Point E_4	0.4994	3.2071	0.0525
Point F_4	0.4999	3.6217	0.0516

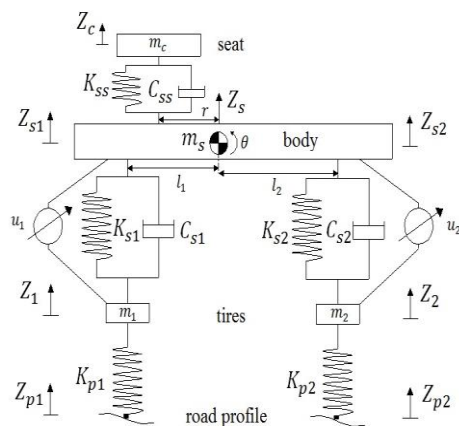


Fig. 15 The Five-degree of freedom vehicle model with active suspension

3.2. Active Model

Fig. 15 shows a five-degree of freedom vehicle suspension model which is a combination of the passive model presented in section 3.1 and two actuators with PID controllers. With similar assumptions, the vehicle velocity has the constant value of $v = 20$ m/s over the

double bumps and also the rear tire moves on the same trajectory of the front tire with a delay of $\Delta t = (l_1 + l_2)/v$. The linear differential equations of motion, with respect to the degree of freedom, can be written as follows. The existence of two signals of two controllers in the following equations is the only difference to motion equations of the passive model in Section 3.1.

$$z_{ps} = z_s - r\theta \tag{17}$$

$$z_{s1} = z_s - l_1\theta \tag{18}$$

$$z_{s2} = z_s + l_2\theta \tag{19}$$

$$F_{ss} = K_{ss}(z_c - z_{ps}) + C_{ss}(\dot{z}_c - \dot{z}_{ps}) \tag{20}$$

$$F_{s1} = K_{s1}(z_{s1} - z_1) + C_{s1}(\dot{z}_{s1} - \dot{z}_1) \tag{21}$$

$$F_{s2} = K_{s2}(z_{s2} - z_2) + C_{s2}(\dot{z}_{s2} - \dot{z}_2) \tag{22}$$

$$m_c \ddot{z}_c = -F_{ss} \tag{23}$$

$$m_s \ddot{z}_s = -F_{s1} - F_{s2} + F_{ss} - u_1 + u_2 \tag{24}$$

$$I_s \ddot{\theta} = l_1 F_{s1} - l_2 F_{s2} - r F_{ss} + l_1 u_1 + l_2 u_2 \tag{25}$$

$$m_1 \ddot{z}_1 = F_{s1} - K_{p1}(z_1 - z_{p1}) + u_1 \tag{26}$$

$$m_2 \ddot{z}_2 = F_{s2} - K_{p2}(z_2 - z_{p2}) - u_2 \tag{27}$$

$$u_1 = k_{p1} e + k_{d1} \frac{de}{dt} + k_{i1} \int e dt \tag{28}$$

$$u_2 = k_{p2} e + k_{d2} \frac{de}{dt} + k_{i2} \int e dt \tag{29}$$

All the parameters except those related to the two controllers are same as the fixed parameters of the passive vehicle model (Section 3.1) whose values were expressed or obtained in the previous section. u_1 and u_2 are the front and rear control signals, respectively. k_{p1} , k_{d1} , and k_{i1} are the front controller parameters. k_{p2} , k_{d2} , and k_{i2} are the rear controller parameters. Z_{p1} and Z_{p2} represent the double bumps excitation of road, as shown in Fig. 10. Note that the design variables of passive model are the fixed parameters in this model. These design variables become fixed by choosing the optimum selected points E_1 , E_2 , E_3 , and E_4 from the related Pareto fronts (in passive model). In the following, $-11000 < k_{p1} < 0$, $-1300 < k_{d1} < 0$, $0 < k_{i1} < 1000$, $0 < k_{p2} < 7000$, $0 < k_{d2} < 80$, and $-5000 < k_{i2} < 0$ are considered as six design variables to be optimally found based on the multi-objective optimization genetic algorithm. Similar to previous section, the objective functions are seat acceleration, front tire velocity, rear tire velocity, relative displacement between sprung mass and front tire, and relative displacement between sprung mass and rear tire.

A population of 80 individuals with a crossover probability of 0.9 and mutation probability of 0.1 has been used in 240 generations.

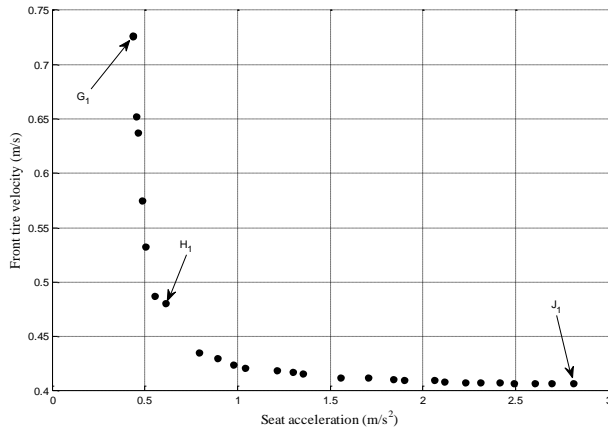


Fig. 16 The Obtained Pareto front of the five-degree of freedom active suspension for seat acceleration and front tire velocity using multi-objective optimization genetic algorithm

Table 9 The values of objective functions and their associated design variables of the optimum points shown in Fig. 16

	k_{p1}	k_{d1}	k_{i1}
Point G_1	-9490.1246	-1073.6773	420.5514
Point H_1	-8737.0233	-842.1452	212.2822
Point J_1	-865.0340	-4.2936	2.1189
	k_{p2}	k_{d2}	k_{i2}
Point G_1	5335.8853	39.3767	-3700.5868
Point H_1	5150.9548	12.9001	-3551.4432
Point J_1	67.5018	0.5961	-137.1680
	$\ddot{z}_c (m/s^2)$	$\dot{z}_1 (m/s)$	
Point G_1	0.4366	0.7266	
Point H_1	0.6107	0.4809	
Point J_1	2.8131	0.4068	

Obtained Pareto fronts of this active model for four pairs of objectives are shown in Figs. 16 to 19, and the values of objective functions and their associated design variables of three optimum points for each figure are given in Tables 9 to 12.

Table 10 The values of objective functions and their associated design variables of the optimum points shown in Fig. 17

	k_{p1}	k_{d1}	k_{i1}
Point G_2	-8979.7508	-1045.4720	494.4313
Point H_2	-6246.8203	-1022.8856	202.2859
Point J_2	-1099.4640	-994.0698	262.8921
	k_{p2}	k_{d2}	k_{i2}
Point G_2	5626.6319	51.3839	-3936.9626
Point H_2	576.2304	67.9625	-4256.9280
Point J_2	6329.0565	48.2684	-3724.0063
	$\ddot{z}_c (m/s^2)$	$\dot{z}_2 (m/s)$	
Point G_2	0.4505	0.4224	
Point H_2	0.8383	0.4209	
Point J_2	1.8872	0.4201	

Table 11 The values of objective functions and their associated design variables of the optimum points shown in Fig. 18

	k_{p1}	k_{d1}	k_{i1}
Point G_3	-9172.3617	-1150.4992	610.5210
Point H_3	-8051.9831	-893.8784	774.6310
Point J_3	-7923.6352	-168.9528	837.0506
	k_{p2}	k_{d2}	k_{i2}
Point G_3	3888.4744	51.0993	-3335.2942
Point H_3	3699.4403	49.5145	-2699.3321
Point J_3	3489.7572	34.8497	-591.9322
	$\ddot{z}_c (m/s^2)$	$d_1 (m)$	
Point G_3	0.8954	0.1324	
Point H_3	1.0857	0.0697	
Point J_3	1.8135	0.0509	

Note that the direction of the signals of the controllers would be changed when the front tire crosses on the bump.

Table 12 The values of objective functions and their associated design variables of the optimum points shown in Fig. 19

	k_{p1}	k_{d1}	k_{i1}
Point G_4	-9456.8099	-1244.6119	639.7846
Point H_4	-8018.3664	-1248.4557	774.1705
Point J_4	-5944.2039	-1249.3697	878.0658
	k_{p2}	k_{d2}	k_{i2}
Point G_4	5363.1819	47.1442	-3335.2942
Point H_4	5636.5207	50.0937	-2699.3321
Point J_4	5697.07880	51.2353	-591.9322
	\ddot{z}_c (m/s ²)	d_2 (m)	
Point G_4	0.5032	0.0576	
Point H_4	0.5838	0.0373	
Point J_4	0.7593	0.0296	

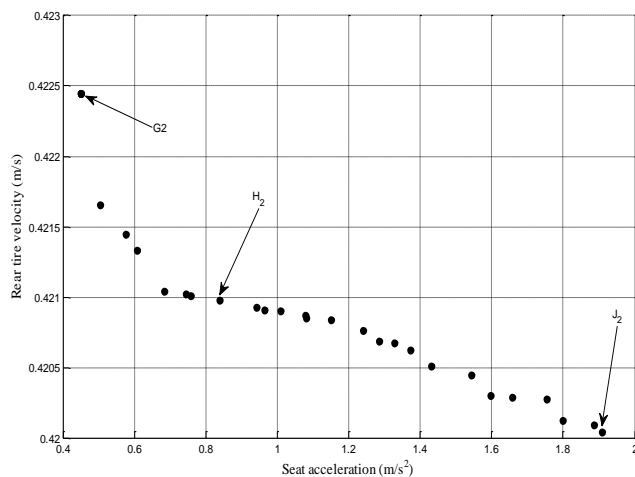


Fig. 17 The Obtained Pareto front of the five-degree of freedom active suspension for seat acceleration and rear tire velocity using multi-objective optimization genetic algorithm

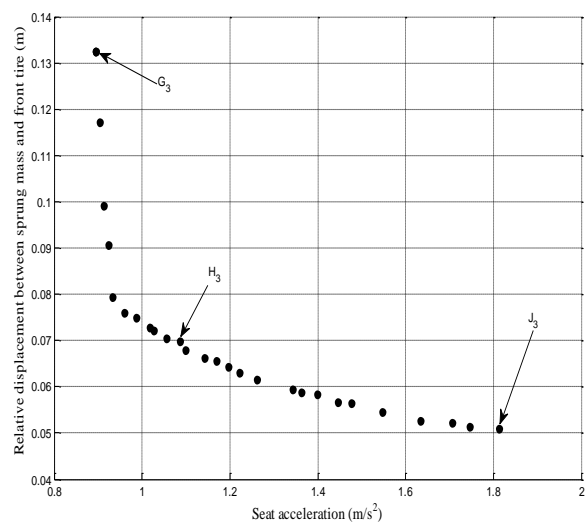


Fig. 18 The Obtained Pareto front of the five-degree of freedom active suspension for seat acceleration and relative displacement between sprung mass and front tire using multi-objective optimization genetic algorithm

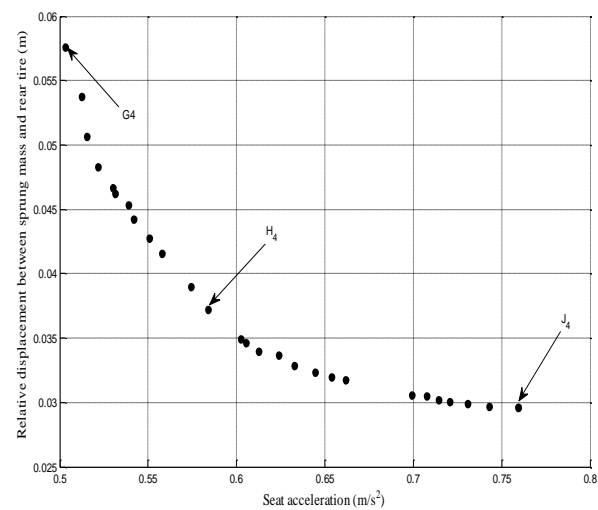


Fig. 19 The Obtained Pareto front of a five-degree of freedom active suspension for seat acceleration and relative displacement between sprung mass and rear tire using multi-objective optimization genetic algorithm

In Figs. 20 to 23, the comparison of the proposed Pareto fronts of the active suspension model with suggested models in [23], [24] is depicted for four pairs of objective functions.

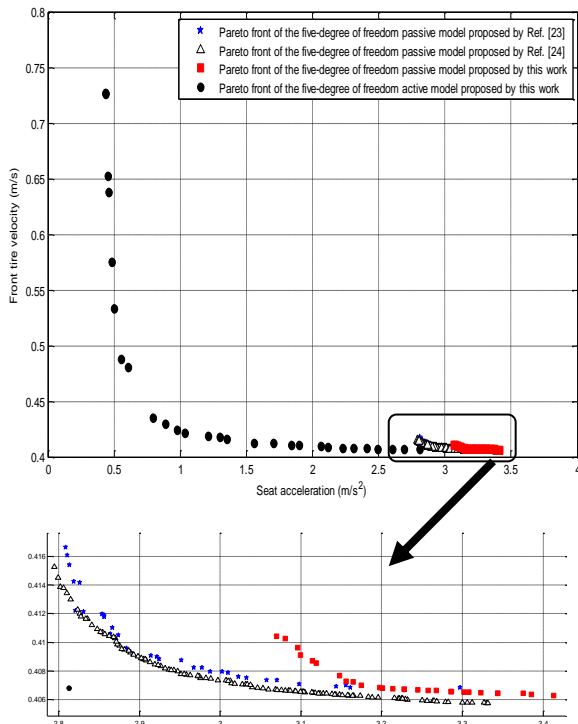


Fig. 20 The comparison of the Pareto fronts obtained by this work and [23], [24] for the five-degree of freedom vehicle model with seat acceleration and front tire velocity as the objective functions

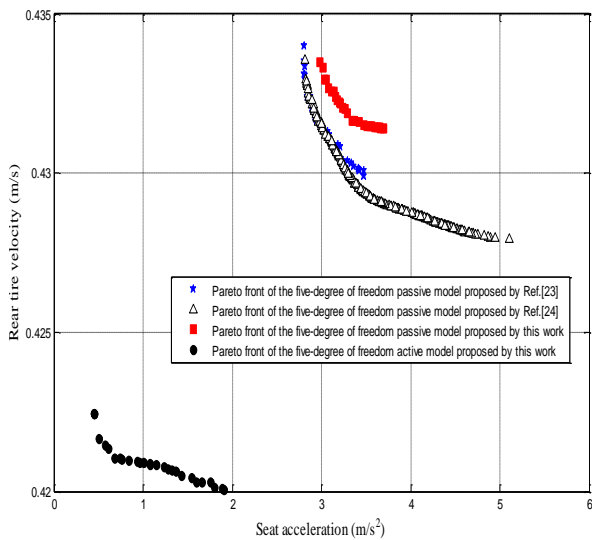


Fig. 21 The comparison of the Pareto fronts obtained by this work and [23], [24] for the five-degree of freedom vehicle model with seat acceleration and rear tire velocity as the objective functions

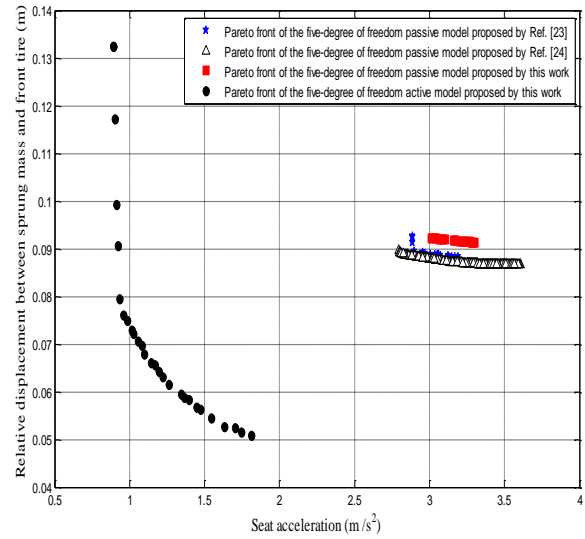


Fig. 22 The comparison of the Pareto fronts obtained by this work and [23], [24] for the five-degree of freedom vehicle model with seat acceleration and relative displacement between sprung mass and front tire as the objective functions

The most important obtained result from Figs. 20 to 23 is the superiority of the active model in comparison with the optimum passive models reported so far. The comparison of the time responses of relative displacement between sprung mass and front (and rear) tire and seat acceleration with proposed models in [10], [23], [24] is depicted in Figs. 24 to 27. Also their values are given in Tables 13 and 14. For this comparison, the equitable points H_3 and H_4 have been chosen from Figs. 18 and 19. Clearly, the proposed active design has a better performance than the models obtained by others.

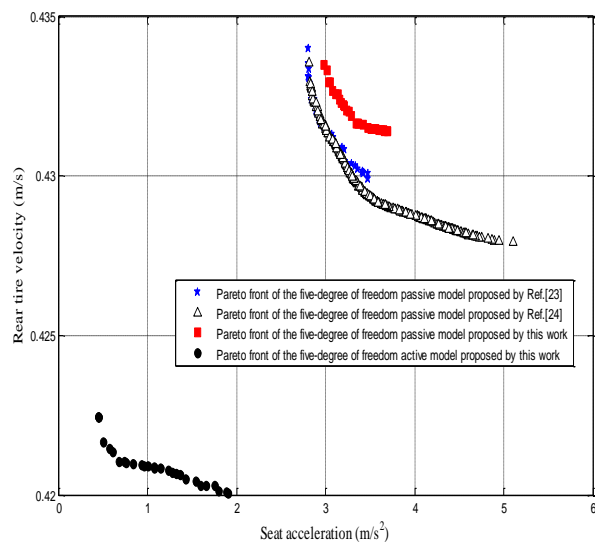


Fig. 23 The comparison of the Pareto fronts obtained by this work and [23,24] for the five-degree of freedom vehicle model with seat acceleration and relative displacement between sprung mass and rear tire as the objective functions

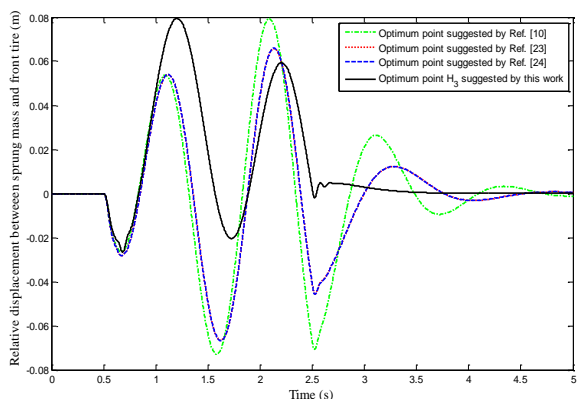


Fig. 24 The Comparison of time responses of relative displacement between sprung mass and front tire for point H_3 by this work and the optimum points proposed in [10], [23], [24]

Table 13 The values of the objective functions for the optimum point H_3 by this work and the optimum points proposed in [10], [23], [24]

	\ddot{z}_c (m/s ²)	d_1 (m)
Point H_3 by this work	1.0857	0.0697
Suggested optimum point in [24]	2.0810	0.0890
Suggested optimum point in [23]	2.8165	0.0892
Suggested optimum point in [10]	4.0981	0.1069

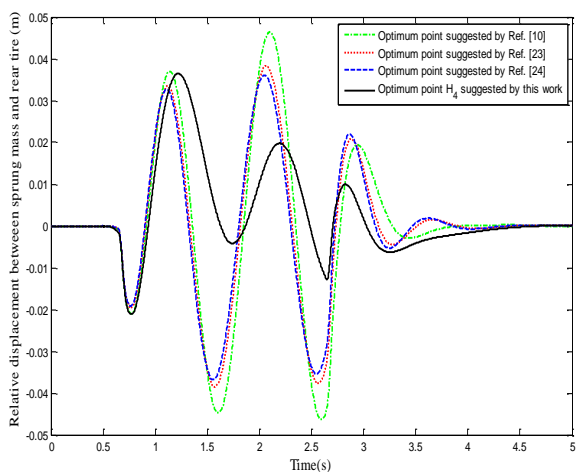


Fig. 25 The Comparison of time responses of relative displacement between sprung mass and rear tire for point H_4 by this work and the optimum points proposed in [10], [23], [24]

The integral of absolute values of time behaviors of the front control force (u_1) and the rear control force (u_2) for the equitable design points H_1 , H_2 , H_3 , and H_4 are given in Table 15.

Table 14 The values of the objective functions for the optimum point H_4 by this work and the optimum points proposed in [10], [23], [24]

	\ddot{z}_c (m/s ²)	d_2 (m)
Point H_4 by this work	0.5838	0.0373
Suggested optimum point in [24]	2.9504	0.0516
Suggested optimum point in [23]	2.9767	0.0534
Suggested optimum point in [10]	4.0981	0.0618

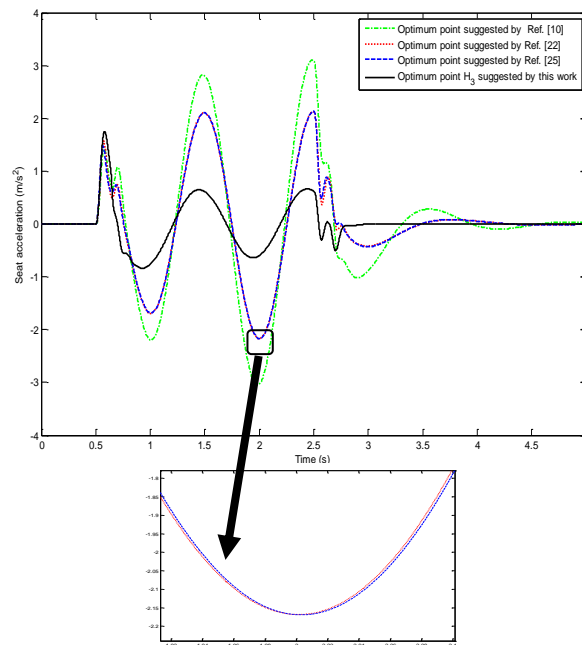


Fig. 26 The Comparison of time responses of seat acceleration for point H_3 by this work and the optimum points proposed in [10], [23], [24]

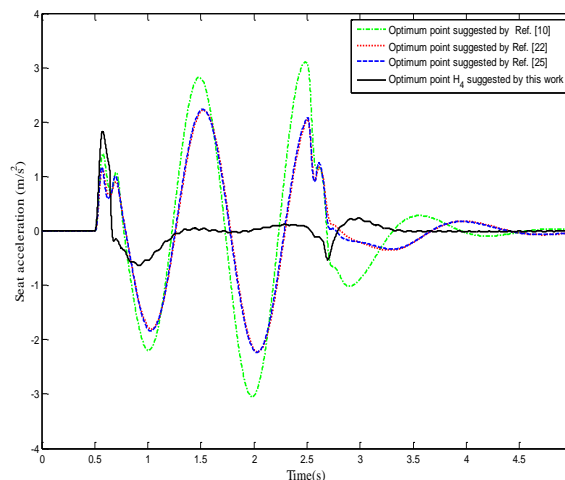


Fig. 27 The Comparison of time responses of seat acceleration for point H_4 by this work and the optimum points proposed in [10], [23], [24]

Table 15 The values of front (u_1) and rear (u_2) control forces

	u_1 (N)	u_2 (N)
Point H ₁	1097.10	1104.60
Point H ₂	950.22	747.70
Point H ₃	867.96	758.48
Point H ₄	1319.70	801.20

4 CONCLUSION

As mentioned, there are several parameters of vehicle ride comfort when designing a suspension system. Some of the more impressive parameters in this study are seat acceleration, relative displacement (and tire velocity for 5-DOF model) by which the optimization has been done over the design variables. It is clear that needing more than one objective to get optimized is why a type of multi-objective optimization that is the multi-objective genetic algorithm (defined in toolbox of MATLAB software) has been used to optimally design the passive car-quarter/car-half model, and active ones. To have an active design of each model, a PID controller has been implemented. Though which controller could be suitably chosen to make performance of a system get better is inherently a controversial problem in this case, how to optimize the chosen controller is equally important after selecting the controller, and this is what has been done in this study to improve the ride comfort. To this end, what is needed is a set of points as the results by which providing appropriate optimal designs can be possible as it is clear from Figs. 5, 18, and 19 which are the results of optimization.

In fact, multi-objective optimization of active models (like passive ones) has led to discovering some important equitable points amongst some conflicting objective functions whose values have been reduced to an acceptable level in comparison with the related references. Most important objectives used in this study are relative displacement, and seat acceleration. The optimization results of two-degree of freedom model prove that the seat acceleration and the relative displacement between sprung mass and tire have been reduced by 32% and 30%, respectively. Moreover, for the five-degree of freedom model, the amount of reduction on the relative displacement between sprung mass and front tire is 22%; on the relative displacement between sprung mass and rear tire is 28% and on the seat acceleration of design points E₃ and E₄ are respectively 48% and 80%. These results show the superiority of the proposed active designs by this work in comparison with the best passive models (two-degree of freedom and five-degree of freedom) published so far.

REFERENCES

- [1] Karnopp, D., "Analytical results for optimum actively damped suspension under random excitation", *Journal of Acoustic Stress and Reliability in Design*, Vol. 111, 1989, pp. 278-283.
- [2] Sun, L., "Optimum design of road-friendly vehicle suspension systems subjected to rough pavement surfaces", *Applied Mathematical Modeling*, Vol. 26, 2002, pp. 635-652.
- [3] Sireteanu, T., Stoia, N., "Damping optimization of passive and semi-active vehicle suspension by numerical simulation", *Proceedings of the Romanian Academy Series A*, Vol. 4, No. 2, 2003, pp. 121-127.
- [4] Sun, L., Cai, X., and Yang, J., "Genetic algorithm-based optimum vehicle suspension design using minimum dynamic pavement load as a design criterion", *Journal of Sound and Vibration*, Vol. 301, 2007, pp. 18-27.
- [5] Y. Sam, J. Osman, M. Ghani, Sliding mode control design for active suspension on a half-car model, in *Proceedings of student conference on research and development*, Putrajaya, Malaysia, 2003, pp. 36-42.
- [6] Cho, J., Jung, T., Kwon, S., and Joh, J., "Development of a fuzzy sky-hook algorithm for a semi-active ER vehicle suspension using inverse model", in *Proceeding of IEEE International Conference on Fuzzy Systems*, Canada, 2006, pp. 1550-1556.
- [7] Griffin, M., Parsons, K., and Whitham, E., "Vibration and comfort IV", *Application of experimental results*, *Ergonomics*, vol. 25, 1982, pp. 721-739.
- [8] Rakheja, S., "Computer-aided dynamic analysis and optimal design of suspension system for off-road tractors", Ph. D. Thesis, Concordia University, Canada, 1985.
- [9] Barak, P., "Magic numbers in design of suspensions for passenger cars", *SAE Technical Paper 911921*, 1991, pp. 53-88.
- [10] Bouazara, M., "Etude et analyse de la suspension active et semi-active des vehicules routiers", Ph.D. Thesis, University Laval, Canada, 1997.
- [11] Hrovat, D., "Optimal active suspensions for 3d vehicle models", in *Proceedings of American Control Conference*, Vol. 2, 1991, pp. 1534-1541.
- [12] Crolla, D. A., "Semi-active suspension control for a full vehicle model", *SAE Technical Paper 911904*, 1992, pp. 45-51.
- [13] Bouazara, M., Richard, M. J., "An optimal design method to control the vibrations of suspension for passenger cars", in *Proceeding of International Mechanical Engineering Congress and Exposition: The Winter Annual Meeting of ASME Atlanta*, 1996, pp. 61-68.
- [14] Bouazara, M., Richard, M. J., "An optimization method designed to improve 3-D vehicle comfort and road holding capability through the Use of active and semi-active suspensions", *European Journal of Mechanics-A/solids*, Vol. 20, No. 3, 2001, pp. 509-520.
- [15] Gündoğdu, U., "Optimal seat and suspension design for quarter car with driver model using genetic algorithms", *International Journal of Industrial Ergonomics*, Vol. 37, No. 4, 2007, pp. 327- 332.
- [16] Alkhatib, R., NakhaieJazar, G., and Golnaraghi, M. F., "Optimal design of passive linear suspension using genetic algorithm", *Journal of Sound and Vibration*, Vol. 275, 2004, pp. 665-691.

- [17] Coello Coello, C. A., Christiansen, A. D., "Multi objective optimization of trusses using genetic algorithms", *Computers and Structures*, Vol. 75, 2000, pp. 647-660.
- [18] Coello Coello, C. A., Van Veldhuizen, D. A., and Lamont, G. B., "Evolutionary algorithms for solving multi-objective problems", New York, Kluwer Academic, 2002.
- [19] Fonseca, C. M., Fleming, P. J., "Genetic algorithms for multi-objective optimization, in: formulation", discussion and generalization, in *Proceedings of Fifth International Conference on Genetic Algorithms*, 1993, pp. 416-42.
- [20] Srinivas, N., Deb, K., "Multi-objective optimization using non-dominated sorting in genetic algorithms", *Evolutionary Computation*, Vol. 2, No. 3, 1994, pp. 221-248.
- [21] Bagheri, A., Mahmoodabadi, M. J., Rostami, H., and Kheybari, S., "Pareto optimization of a two-degree of freedom passive linear suspension using a new multi-objective genetic algorithm", *International Journal of Engineering*, Vol. 24, No. 3, 2011, pp. 291-299.
- [22] Rajeswari, K., Lakshmi, P., "PSO optimized fuzzy logic controller for active suspension system", in *Proceeding of International Conference on Advances in Recent Technologies in Communication and Computing*, Kottayam, Kerala India, 2010, pp. 278-283.
- [23] Nariman-zadeh, N., Salehpour, M., Jamali, A., and Haghgoo, E., "Pareto optimization of a five-degree of freedom vehicle vibration model using a multi-objective uniform-diversity genetic algorithm (MUGA)", *Engineering Applications of Artificial Intelligence*, Vol. 23, 2010, pp. 543-551.
- [24] Mahmoodabadi, V., Safaie, A. A., Bagheri, A., and Nariman-zadeh, N., "A novel combination of particle swarm optimization and genetic algorithm for Pareto optimal design of a five-degree of freedom vehicle vibration model", *Applied Soft Computing*, Vol. 13, No. 5, 2013, pp. 2577-2591.
- [25] Sharifi, M., Shahriari, B., and Bagheri, A., "Optimization of sliding mode control for a vehicle Suspension System via Multi-objective Genetic Algorithm with Uncertainty", *Journal of Basic and Applied Scientific Research*, Vol. 2, No. 7, 2012, pp. 6724-6729.
- [26] Vahidi, A. Eskandarian, A., "Predictive Time-Delay Control of Vehicle Suspensions", *Journal of Vibration and Control*, Vol. 7, No.8, 2001, pp. 1195-1211.
- [27] Baumal, A. E. Mcphee, V., and Calamai, P. H., "Application of genetic algorithms to the design optimization of an active vehicle suspension system", *Computer Methods in Applied Mechanics and Engineering*, Vol. 163, No. (1-4), 1998, pp. 87-94.
- [28] Thoresson, M. J., Uys, P. E., Els, P. S., and Snyman, J. A., "Efficient optimisation of a vehicle suspension system using a gradient-based approximation method", Part 1: Mathematical Modelling, *Mathematical and Computer Modelling*, Vol. 50, No. (9-10), (2009), pp. 1421-1436.
- [29] Crews, J. H., Mattson, M. G., and Buckner, G. D., "Multi-objective control optimization for semi-active vehicle suspensions", *Journal of Sound and Vibration*, Vol. 330, No. 23, 2011, pp. 5502-5516.
- [30] Guo, D. L., Hu, H.Y., and Yi, J. Q., "Neural network control for a semi-active vehicle suspension with a magnetorheological damper", *Journal of Vibration and Control*, Vol. 10, No. 3, 2004, pp. 461-471.
- [31] Eski, I., Yildirim, S., "Vibration control of vehicle active suspension system using a new robust neural network control system", *Simulation Modelling Practice and Theory*, Vol. 17, No. 5, 2009, pp. 778-793.
- [32] Mao, X., Wang, Q., "Delay-dependent control design for a time-delay supercavitating vehicle model", *Journal of Vibration and Control*, Vol. 17, No. 3, 2011, pp. 431-448.
- [33] Nath, T., Kumar, S., "Quarter/Half/Full car models for active suspension (with PID controller)", in *Proceeding of International Conference on Recent Trends in Engineering and Technology*, 2012, pp. 286-290.
- [34] Fayyad, S. M., "Constructing control system for active suspension system", *Contemporary Engineering Sciences*, Vol. 5, No. 4, 2012, pp. 189-200.
- [35] Yagiz, N., Sakman, L. E., "Robust Sliding Mode Control of a Full Vehicle without Suspension Gap Loss", *Journal of Vibration and Control*, Vol. 11, No. 11, 2005, pp. 1357-1374.
- [36] Haiping, D., Nong, Z., and James, L., "Parameter-dependent input-delayed control of uncertain vehicle suspensions", *Journal of Sound and Vibration*, Vol. 317, No. (3-5), 2008, pp. 537-556.